Large-Sample Evaluation of Two Methods to Correct Range-Dependent Error for WSR-88D Rainfall Estimates

BERTRAND VIGNAL AND WITOLD F. KRAJEWSKI

Iowa Institute of Hydraulic Research, The University of Iowa, Iowa City, Iowa

(Manuscript received 26 July 2000, in final form 20 March 2001)

ABSTRACT

The vertical variability of reflectivity is an important source of error that affects estimations of rainfall quantity by radar. This error can be reduced if the vertical profile of reflectivity (VPR) is known. Different methods are available to determine VPR based on volume-scan radar data. Two such methods were tested. The first, used in the Swiss Meteorological Service, estimates a mean VPR directly from volumetric radar data collected close to the radar. The second method takes into account the spatial variability of reflectivity and relies on solving an inverse problem in determination of the local profile. To test these methods, two years of archived level-II radar data from the Weather Surveillance Radar-1988 Doppler (WSR-88D) located in Tulsa, Oklahoma, and the corresponding rain gauge observations from the Oklahoma Mesonet were used. The results, obtained by comparing rain estimates from radar data corrected for the VPR influence with rain gauge observations, show the benefits of the methods—and also their limitations. The performance of the two methods is similar, but the inverse method consistently provides better results. However, for use in operational environments, it would require substantially more computational resources than the first method.

1. Introduction

Different sources of error affect radar rainfall estimates. These sources of error are well known (see, e.g., Zawadzki 1982; Austin 1987; Smith et al. 1996). To derive accurate rainfall estimates from radar measurements for meteorological or hydrological applications, the sources of systematic errors, or biases, should be considered, and the errors corrected. In particular, one has to deal with the sources of range-dependent bias. Evaluation of methods for reducing range-dependent bias, which arises from the vertical variability of the reflectivity profile, is the central theme of our paper.

The nonhomogeneous vertical structure of radar echoes is an important source of range-dependent bias in rainfall estimation using data collected by the Weather Surveillance Radar-1988 Doppler (WSR-88D), as has been documented by Smith et al. (1996) and Fulton et al. (1998). The vertical structure of radar echoes is related to phase changes of hydrometeors and the evolution of their size and shape distribution. The sampling geometry of the radar beam (for WSR-88D it is nominally 0.5° for the base-scan elevation angle and 1° for the 3-dB beamwidth) associated with this vertical structure of radar echoes leads to biases in radar rainfall estimates that are range dependent. To mitigate the effects of this source of error in WSR-88D rainfall estimates, a corrective scheme is needed.

A common approach to this problem consists of estimating a function describing the evolution versus altitude of the radar reflectivity: the vertical profile of radar reflectivity (VPR). This VPR is then used to extrapolate radar reflectivity data aloft to ground level. The literature offers a number of procedures for VPR estimation. Andrieu and Creutin (1995) and Andrieu et al. (1995) solved the inverse problem of retrieving mean VPR at hourly intervals from radar measurements recorded at two elevation angles using discrete inverse theory. Joss and Lee (1995) explored the case of VPR estimation in the difficult context of a mountainous region. Mean VPR is deduced in real time from radar data recorded at 20 elevation angles within a radius of 70 km from the radar. Kitchen et al. (1994) proposed to retrieve an ''idealized'' VPR for each pixel of the radar domain using radar data, surface observations, and infrared satellite data. Smyth and Illingworth (1998) proposed an extension of that work to explore the cases of more complex situations in which convective cells are embedded in large stratiform precipitation areas. Their procedure is based on the discrimination between stratiform and convective precipitation. The method proposed by Kitchen et al. (1994) is applied to correct echoes classified as stratiform, whereas a climatologically based profile is used for echoes classified as con-

Corresponding author address: Dr. Witold F. Krajewski, Iowa Institute of Hydraulic Research, 300 South Riverside Drive, Rm. 404, Iowa City, IA 52242-1585.
E-mail: witold-krajewski@uiowa.edu

vective rain. Vignal et al. (1999) proposed a generalization of the VPR retrieval procedure method proposed by Andrieu and Creutin (1995) to radar data recorded at many elevation angles. This generalization makes it possible to identify VPRs locally, typically at a scale of 20 km by 20 km.

For this study, we selected two different methods to correct the VPR influence: 1) mean VPR (MVPR), obtained from radar data collected close to the radar (e.g., within a range of 100 km and 2) local VPR (LVPR), deduced from radar data for small regions using an inverse method. The MVPR, the principles of which are described by Joss and Lee (1995), allows the actual information on the vertical structure of the radar echoes provided by radar data to be taken into account. A version of this method is used operationally by the Swiss Meteorological Service. The LVPR, proposed by Vignal et al. (1999), allows the variations in space of the VPR to be taken into account. We selected these two methods because (1) their formulations are independent of storm type; and (ii) they are easy to implement with WSR-88D radar data.

Both methods have been evaluated before. Joss and Lee (1995) showed the benefits of the MVPR for rainfall-rate estimation. Vignal et al. (2000) conducted a limited (based on only nine rain events) comparison of these two methods in the context of the Swiss radar network. The study indicates that the LVPR method, by taking into account the variability in horizontal space of the VPRs, resulted in improved accuracy of rainfall estimates from radar as compared with the MVPR method.

In this paper, we present another evaluation of the two methods, this time based on a large sample of radar data collected by the Tulsa, Oklahoma, WSR-88D, mainly during the warm season. We consider that, because of the differences of the rainfall regimes between Switzerland and Oklahoma, as well as different radar characteristics, including the scanning strategy, the results obtained earlier by Vignal et al. (2000) may not be easily transferable. Our large-sample study mimics an operational application and, as such, allows a comprehensive and rigorous evaluation of the benefits and limitations of each method.

There are two elements in our study. First, we develop a validation methodology suitable for evaluation of the VPR correction methods; second, we compare the benefits and limitations of each method using a variety of criteria. Our validation methodology uses two years of radar data from the WSR-88D located in Tulsa and an accompanying database of rain gauge observations used to evaluate the improvement of rain quantity estimates associated with the corrections. The choice of our test location is particularly challenging, considering the varied precipitation regimes over Oklahoma: it is dominated by midlatitude convective systems, but with significant stratiform rainfall contributions. As a by-product of our study, we obtained a climatological VPR for northeast Oklahoma.

This paper is organized as follows. We devote section 2 to formulating the problem and to the methods used to estimate the VPRs. In section 3, we deal with the database and with implementing the VPR estimation methods. In section 4 we present the VPR variability, and in section 5 we discuss an evaluation of the VPR correction methods.

2. Formulation of the problem and VPR estimation methods

a. Formulation of the problem

At each range, the radar measurement integrates the reflectivity over a section of the radar beam. A simplified expression of the radar measurement, assuming horizontally homogeneous reflectivity over the sample volume, can be written as

$$\overline{Z}(x, \alpha) = \int_{H^-(\theta_0,\alpha,x)}^{H^+(\theta_0,\alpha,x)} f^2(\theta_0, h) Z(x, h)\, dh, \qquad (1)$$

where

$$\overline{Z}(x, \alpha)$$

is the reflectivity measured by the radar at the location x; α is the elevation angle; $Z(x, h)$ is the reflectivity at location x and altitude h; H^+ and H^- represent, respectively, the upper and lower limits of the radar beam; and f represents the one-dimensional power distribution of the radar beam at altitude h, which depends on the beam width θ_0. The rainfall rate R is deduced from the reflectivity through the use of a Z–R relationship.

We assume that the function $Z(x, h)$ can be factorized according to the following form:

$$Z(x, h) = Z(x, 0) z_D(h), \qquad (2)$$

where $Z(x, 0)$ represents the radar reflectivity field at the ground level, and the dimensionless factor $z_D(h)$ is called the vertical profile of reflectivity (hereinafter VPR). The VPR is assumed to be homogeneous within the geographic domain D and to be representative of the vertical variations of reflectivity in this domain. Relation (1) can now be written as

$$\overline{Z}(x, \alpha) = Z(x, 0) z_{Da}(x, \alpha), \qquad (3)$$

where we define $Z_{Da}(x, \alpha)$ as

$$z_{Da}(x, \alpha) = \int_{H^-(\theta_0,\alpha,x)}^{H^+(\theta_0,\alpha,x)} f^2(\theta_0, h) z_D(h)\, dh. \qquad (4)$$

Correcting the VPR influence can be easily achieved using (3) if the VPR is known. A correction factor is applied multiplicatively to each radar measurement. Considering rain-rate measurement (rainfall rate deduced from the reflectivity through the use of a Z–R relationship), this correction factor is expressed as

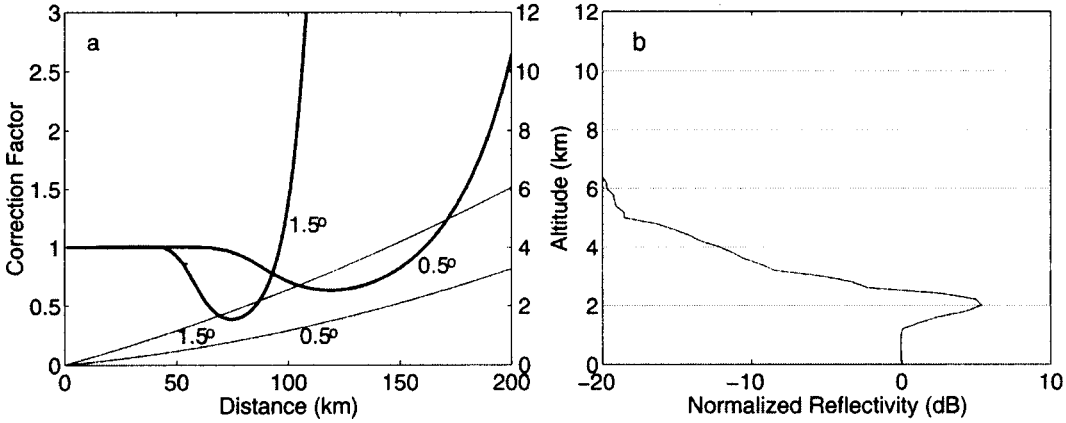

FIG. 1. (a) Illustration of VPR correction curves for two elevation angles associated with (b) an arbitrary vertical profile of reflectivity. In (a), the light lines show the altitude of the beam axis, and the dark lines are the correction factors.

$$P(x, \alpha) = \left[\frac{1}{z_{Da}(x, \alpha)}\right]^{1/b}, \tag{5}$$

where $P(x, \alpha)$ is the correction factor to be applied to the rain rate measured by the radar at location x, and b is the exponent of the Z–R relationship.

The magnitude of this correction is illustrated by an example shown in Fig. 1a. The VPR (Fig. 1b) has a reflectivity peak at an altitude of 2.0 km, above which the reflectivity decreases to −20 dB at an altitude of 6.5 km. This VPR is representative of a cold cloud leading to a marked bright band caused by the melting of ice particles. The correction factors versus range, related to this VPR, are shown in Fig. 1a. We show two curves for the elevation angle of 0.5° and 1.5°. The beamwidth $\theta_0 = 1°$, and the exponent $b = 1.4$ (WSR-88D default Z–R relationship). For the 0.5° case, the correction factor is lower than 1 when the radar beam intersects the melting layer (between 70 and 160 km). The correction factor is greater than 1 when the radar beam is above the melting layer (between 160 and 200 km). Without correction, radar rainfall estimates are overestimated between 70 and 160 km and underestimated at farther ranges.

b. Estimation of MVPR

The mean profile is directly obtained by averaging radar data collected within a 100-km radius at different altitudes. The range is restricted to 100 km to avoid the smoothing effects of the radar beam. In addition, in Switzerland this restriction is also motivated by problems of beam blocking. The mean profile is then used to correct the radar data over the whole radar domain. If not enough rain is recorded close to the radar, a climatological profile is used instead. Further details about this procedure, used operationally in Switzerland, can be found in Joss and Lee (1995).

c. Estimation of LVPR

In this section we briefly summarize the VPR identification algorithm proposed by Vignal et al. (1999). The initial version of this method, proposed by Andrieu and Creutin (1995), retrieves VPR from radar data recorded at two elevation angles. Vignal et al. (1999) generalized it to include data from more elevation angles available in voluminal radar scans.

According to the method, LVPRs are identified in areas of about 20 km by 20 km. Vignal et al. (1999) showed that these local profiles differ from the ''true'' ones because of the smoothing effect of the radar beam when the region of analysis is farther than 50 km from the radar. It is inappropriate to correct radar data using such profiles. Clearly, a procedure for retrieval of the true profile is required.

The main assumption of the method is that the VPR is homogeneous in the region of analysis, which permits separation of horizontal and vertical variations of the reflectivity [(2)]. The ratio of two radar data, expressed in rainfall intensity, observed at a given location and at two different elevation angles can be written as follows:

$$q_R(x, \alpha_1, \alpha_i) = \left[\frac{z_{Da_i}(x, \alpha_i)}{z_{Da_1}(x, \alpha_1)}\right]^{1/b}, \quad \text{for } i = 2, 3, \ldots, 9, \tag{6}$$

where $q_R(x, \alpha_1, \alpha_i)$ is the intensity ratio measured at the distance x, and α_1 and α_i are the elevation angles (α_1 being the lowest one).

The ratio allows filtering the horizontal variations of the radar reflectivity at ground, where the intensity ratio depends only on the radar beam and the VPR characteristics. In the region of analysis, by averaging these ratios over azimuth, average ratio versus distance is obtained. Considering the distance interval associated with the region of analysis, a ratio curve becomes a characteristic of the VPR. In Fig. 2 we show an example of

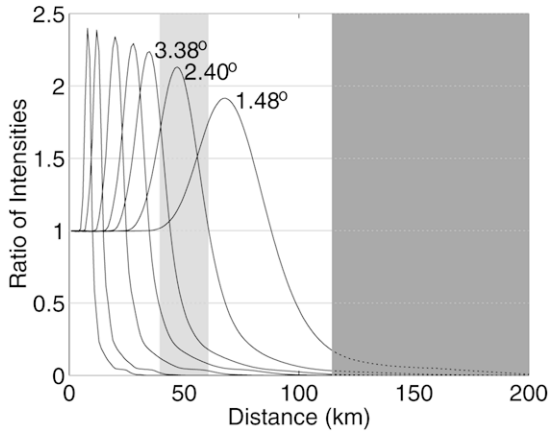

FIG. 2. Example of ratio curves of radar data simulated using the VPR shown in Fig. 1b. The light-shaded region corresponds to one 20-km interval used in LVPR-correction calculations. The dark-shaded region denotes distance over which no VPR corrections should be made, because the lowest angle (0.5°) is no longer a good reference.

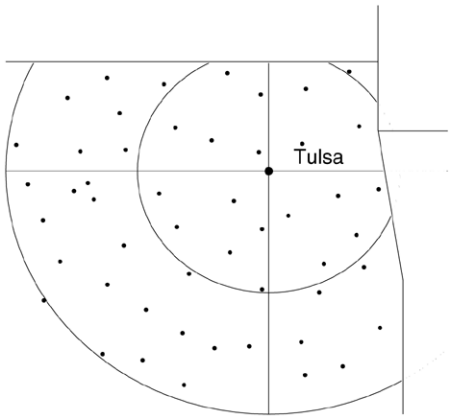

FIG. 3. Locations of the Oklahoma Mesonet rain gauges used in this study (circles indicate 100- and 200-km range from radar site). Only the Oklahoma part of the radar umbrella is shown.

the set of ratio curves in a distance interval 40–60 km. We simulated these curves using the theoretical model in (5) and an arbitrary VPR shown in Fig. 1b. Variations of ratios with distance are due to the increase of the beam height with range. Differences between two ratio curves are due to the different elevation angles considered. A set of ratio curves can be considered as the signature of the VPR in the region of analysis. The light shaded region corresponds to a range used in LVPR estimation, and the dark shaded region denotes the range over which the 0.5° is no longer a good reference, because the radar beam intercepts the bright band.

The objective of the identification method is to determine the VPR consistent with observed ratio curves. To perform this identification, different elements are available: (i) the set of ratio curves, (ii) the theoretical model in (5) relating the ratios and the VPR, and (iii) the radar data–based VPR. The VPR identification consists of determining the VPR, which leads through (5) as closely as possible (in the sense of least squares fit) to the observed ratio curves. To solve this inverse problem (Menke 1989), we used the algorithm proposed by Tarantola and Valette (1982a,b). We initialize this algorithm using the local VPR directly deduced from voluminal radar data. For details see Andrieu and Creutin (1995) and Andrieu et al. (1995).

Vignal et al. (1999) showed that this procedure allows effective identification of the VPRs by range intervals. As a consequence, to apply this method, we divide the radar domain into several regions of analysis. For each region of analysis, we compute the ratio curves of radar data. We use these ratio curves to identify the local VPR. The LVPR is then used to correct the radar data for the given region.

3. The database and application conditions of the VPR estimation methods

We test the effectiveness of correcting the range-dependent errors in radar reflectivity using two years (1994 and 1995) of volumetric data from the Tulsa WSR-88D. First, the radar data were converted from the archived level-II format (Klazura and Imy 1993) to the more efficient format developed by Kruger and Krajewski (1997). To improve the quality of the data, we applied the anomalous propagation echo detection method developed by Grecu and Krajewski (1999). We document the results in Krajewski and Vignal (2001).

For the WSR-88D radars, the 3-dB beamwidth is 1°. In precipitation mode, the radar performs a full volume scan every 6 min. Nominally, each volume scan is composed of nine scans at elevation angles increasing from 0.5° to 19.5° for a range of 230 km (truncated to 200 km in our database). We converted radar measurements Z into rainfall intensities R using the WSR-88D default relationship, $Z = 300R^{1.4}$. We also used the Oklahoma Mesonet (Brock et al. 1995) data to calculate hourly rainfall accumulations at 49 locations within the radar domain (Fig. 3). Basic quality control for these data is carried out by the Oklahoma Climatological Survey (Shafer et al. 2000). The precipitation regime for the region is dominated by midlatitude convective systems (Houze et al. 1990; Houze 1993).

To simulate properly an operational application of the procedure using mean profile, a climatological VPR has to be estimated first. We estimated a climatological VPR by using two years of the radar observed profiles and averaging them, with weights being the mean rainfall intensity over the region of analysis (range of 100 km from the radar). This profile (described later in displays a peak of reflectivity (+2.5 dB) at height of 2.8 km. This altitude can be interpreted as the mean level of the bright band. Above, the reflectivity decreases linearly with altitude at the rate of 2 dB km^{-1}.

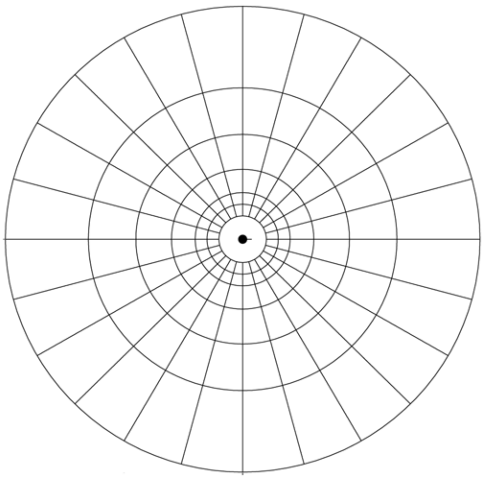

FIG. 4. Regions of analysis used to estimate locally identified VPRs (azimuth sectors are 15° wide; circles indicate 20-, 30-, 40-, 60-, 90-, 130-, and 200-km range from radar site).

Vignal et al. (1999) performed an investigation of the appropriate conditions of LVPR identification. The study led to the following conclusions: (i) VPR can be correctly identified by range intervals, (ii) the accuracy decreases when the range interval is far from the radar, and (iii) the range interval must be increased with distance to retrieve the VPR with the same efficiency as for closer ranges. Following the method of Vignal et al. (1999), we divided the radar domain into 144 regions of analysis as illustrated in Fig. 4. Each region of analysis is 15° wide in azimuth, and the radial extent increases with distance from the radar, ranging from 10 to 70 km. For numerical reasons, we estimated discrete VPR with a $\Delta h = 0.2$ km step. For both methods, we estimated hourly VPRs.

4. The VPRs

a. The MVPRs

We obtained 410 MVPRs by analyzing over 1000 hours of data. We show a subset of these in Fig. 5. These VPRs exhibit a wide range of behavior. However, they have several features in common. First, the reflectivity is nearly constant in the lowest 2 km above the ground. Second, many of the VPRs display an enhancement of the reflectivity (up to 9.5 dB) at a certain height. Most of the time, it can be associated with the presence of stratiform precipitation. The altitude of this bright band differs from one VPR to another but typically is at about 2 km in March and 3.5 km in July. Third, at higher levels (above 4 km) the reflectivity decreases with increasing altitude. This decrease of the reflectivity varies from -7 to -1 dB km^{-1}. When a strong enhancement of the reflectivity is observed, the reflectivity decreases faster above 4 km than in the absence of a strong enhancement.

These VPRs explain qualitatively the bias observed between rainfall accumulation from radar and from rain gauges (see section 5). Considering rainfall accumulation deduced from radar data recorded at an elevation angle of 0.5°, no important bias is observed up to a distance of 100 km. For this range, the altitude of the beam axis is below 1.5 km. Between 100 and 200 km, radar estimates are biased positively. The altitude of the beam axis lies between 1.5 and 4 km. If we consider rainfall accumulation deduced from radar data recorded at an elevation angle of 1.5°, no important bias is observed from the radar up to only 50 km (the altitude of the beam axis is above 1.5 km). Radar rainfall accumulations are overestimated from 50 to about 120 km where the altitude of the beam axis is between 1.5 and 4 km. At farther distances, radar rainfall accumulations are underestimated.

We have to recognize that these MVPRs only provide an incomplete perception of the variability of the VPRs. As a consequence, for example, these VPRs incorrectly represent cases in which convective cells are embedded in larger stratiform precipitation regions.

b. The LVPRs

Locally identified VPRs provide better information on the variability in time and space of the VPRs. Figure 6 illustrates the variations in time and space of the VPR at the scale of a rain event. We show (Fig. 6a) hourly accumulations estimated from the lowest plan position indicator (elevation angle of 0.5°) for the event of 8 May 1995 at 0300 LST. High spatial variability is evident in the rain amounts obtained for this hour over the radar domain. This example is typical of the rainfall regime in Oklahoma, where convective cells produce areas of high rain amount while large areas of more stratiform rain produce weaker rain amount. The associated VPRs obtained for this hour between the range of 60 and 90 km are presented in Fig. 6b. Two groups of VPRs can be distinguished. The first group (S) is typical for stratiform rain (strong brightband enhance-

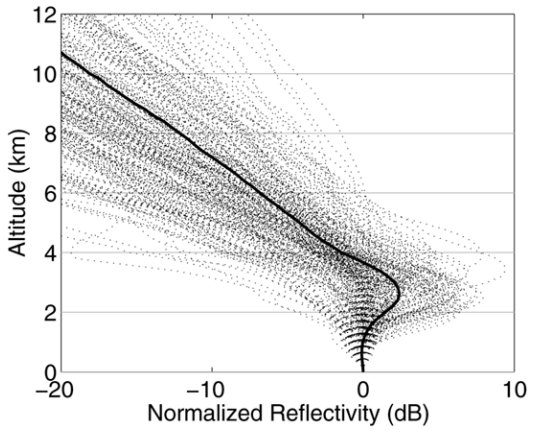

FIG. 5. Two-year sample of the MVPRs and the climatological VPR (thick line).

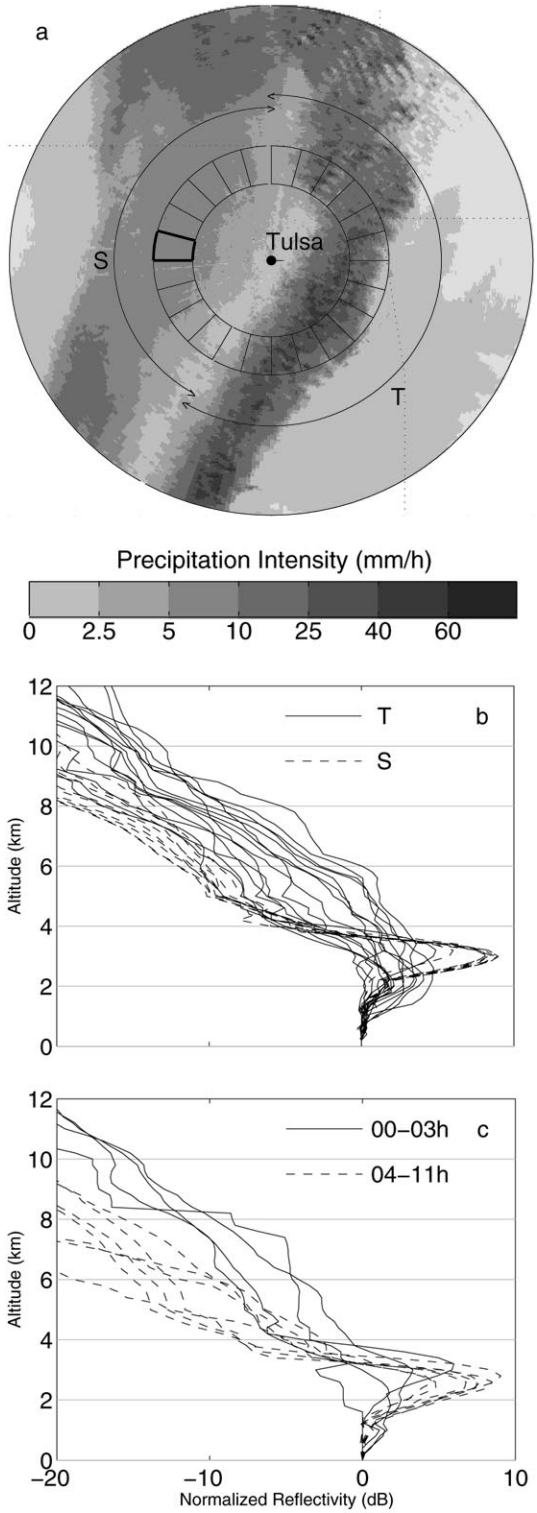

ment and fast decrease of the reflectivity above it). We notice than the VPRs taken at different locations are similar to each other. The bright band is at an altitude of 2.8 km and is associated with an enhancement of +9 dB. Above this bright band the decrease of the reflectivity with height is at the rate of about -4 dB km^{-1}. The second group of VPRs (T) is typical for convective cells and regions of transition between stratiform and convective rain. Some of these profiles are similar to the previous one, whereas others display no bright band and a weaker negative gradient (-3 dB km^{-1}). In general, we observe greater variability of VPR in this group.

Let us compare these VPRs with those obtained at a single location over a period of time. The VPRs obtained between 60 and 90 km and 270°–285° in azimuth, from 11 h of rain, are presented in Fig. 6c. This set of VPRs is very similar to the one presented in Fig. 6b.

In Fig. 7 we show the space–time variability of the LVPRs based on 2 yr of data. The VPRs presented, obtained between 60 and 90 km, correspond to different accumulations of average area rainfall. For the VPRs shown in Fig. 7a, the averaged hourly accumulation is between 1.75 and 2.25 mm; for the VPRs shown in Fig. 7b, the averaged hourly accumulation is between 9.5 and 10.5 mm. For both cases, we observe a wide range of VPR behavior. When the mean hourly rainfall accumulation is increasing, we see a tendency of VPRs to decrease less with height. The averaged VPRs shown in Figs. 7a,b illustrate this point. At the same time, the probability of bright band is greater for weak mean rainfall accumulation (35% of the profiles exhibit an enhancement greater the +3 dB) than for larger mean rainfall accumulation (26% of the profiles exhibit an enhancement greater than +3 dB).

These observations indicate that for weak mean rainfall accumulations the VPRs are more typical for stratiform rain and larger accumulations correspond to convective conditions. However, this is only true on average. For low mean rainfall accumulation, a weak decrease of the reflectivity with height without brightband enhancement can be observed, whereas for large mean rainfall accumulation, some profiles are characterized by a rapid decrease of the reflectivity with height and a localized strong enhancement of the reflectivity.

5. Evaluation of the two methods

In this section we evaluate radar rainfall estimates considering 1) radar data only and 2) radar–gauge comparison. In addition to considering radar rainfall estimates from radar data recorded at an elevation angle of 0.5°, we also used 1.5° and 2.5°. This allows some gen-

←

FIG. 6. Illustration of the variability in time and space of the LVPRs. (a) Hourly mean rain rate from radar data recorded at 0.5° (0300 LST 8 May 1995); also shown are 24 sectors selected for illustrating the variability in space of the VPR. (b) Corresponding LVPRs, divided into two groups [group S corresponds to area of stratiform rain, group T corresponds to convective rain as marked in (a)]. (c) Time series of the VPRs obtained over the bold-marked sector divided into two groups according to time during the same storm.

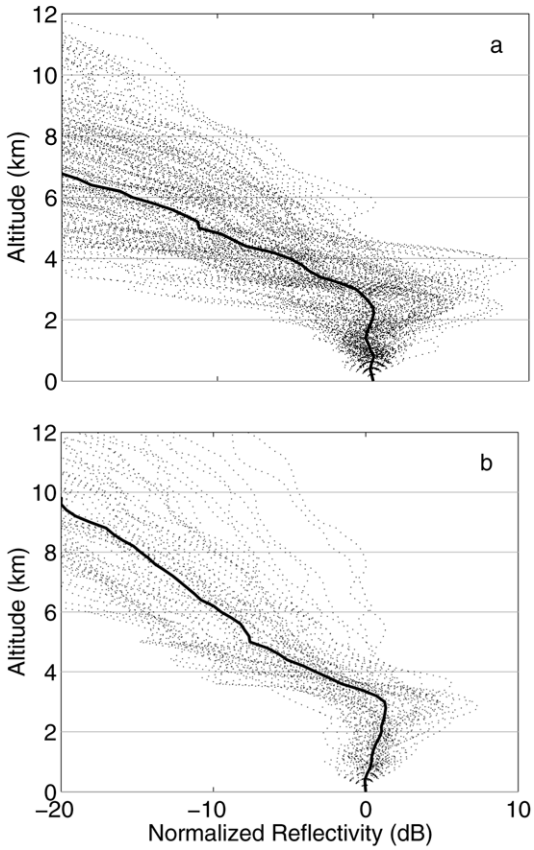

FIG. 7. Conditional sample of locally identified VPRs obtained between 60 and 90 km from the radar. (a) VPR obtained on region of analysis for which radar data at 0.5° reported an average rainfall between 0.75 and 1.25 mm h^{-1}. (b) VPR obtained on region of analysis for which radar data at 0.5° reported an average rainfall between 9.50 and 10.50 mm h^{-1}.

eralization of our results for a situation in which hybrid scans have to be constructed to form a radar rainfall map.

a. Evaluation using radar data only

This evaluation is performed considering radar rainfall accumulation over the two years of data. Figure 8 shows (i) the uncorrected, (ii) the corrected using the MVPR, and (iii) the corrected using the LVPR radar rainfall accumulation (mm). Such long-duration maps are useful in identifying range biases that cannot be detected if short-duration maps are used, because of large natural variability of rainfall. These figures show that, even considering two years of rainfall accumulation, natural variability of rainfall is important. A gradient of rain amount (from the northwest of the radar umbrella with the lower rain amounts to the southern one with higher rain amounts) is observed. A similar trend is evident for rain amount from gauges. Also visible is partial beam blockage, especially in the northeastern part of the radar domain (see Fig. 8a). The im-

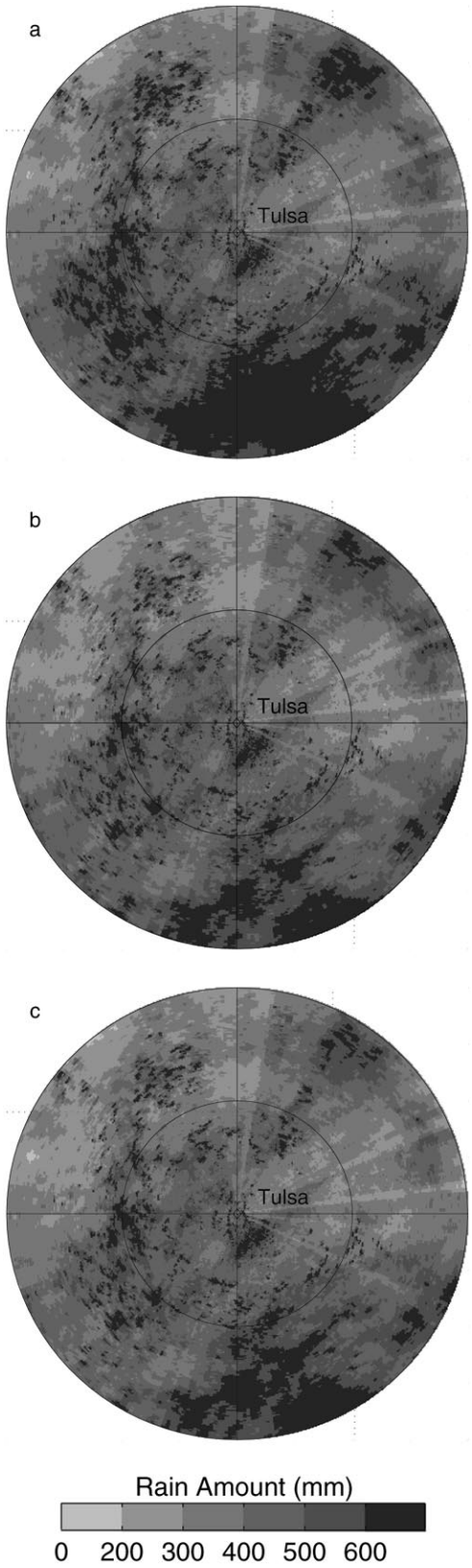

FIG. 8. Two-year accumulation map based on radar data recorded at an elevation of 0.5° (a) without VPR correction, (b) corrected using MVPR, and (c) corrected using LVPR.

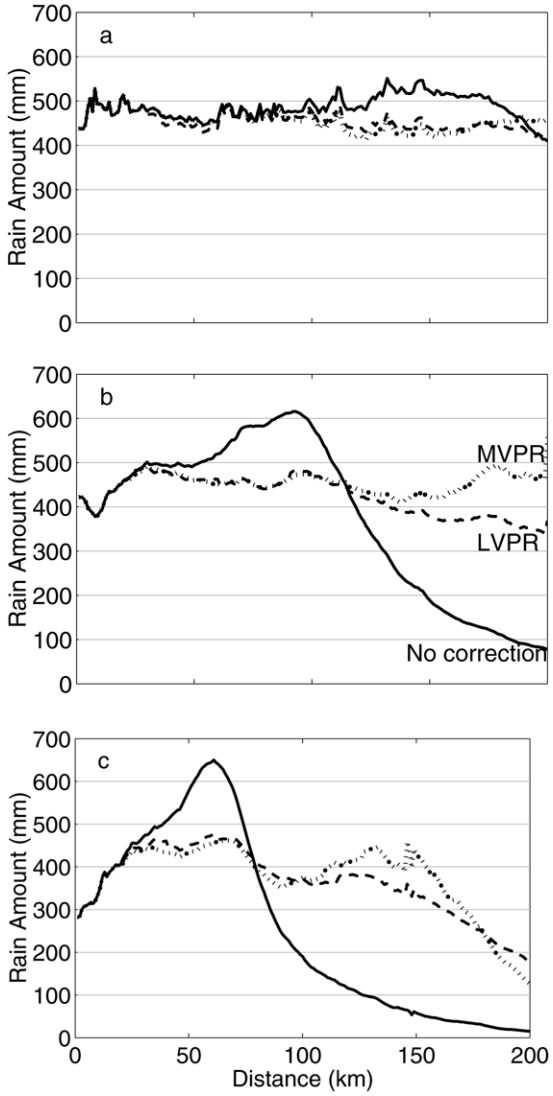

FIG. 9. Azimuthally averaged 2-yr accumulation based on radar data recorded at (a) 0.5°, (b) 1.5°, and (c) 2.5°. Continuous lines are for radar data without VPR correction, dotted lines are for radar data corrected using MVPRs, and mixed lines are for radar data corrected using LVPRs.

pact of both VPR corrections is significant at ranges greater than 150 km in the southern part of the radar domain. Considering radar data recorded at higher elevation angles (1.5° and 2.5°), the impact of the VPR correction is more evident because the VPR influence is more significant.

To complete this analysis of total accumulation, let us consider azimuthally averaged radar rainfall accumulations (Fig. 9). We assumed that the mean rainfall over time does not depend on distance, and thus the range dependence of the mean radar rainfall accumulations is induced by radar estimation error. The solid line in Fig. 9a is for rainfall accumulation from radar data recorded at 0.5° without VPR correction, the dotted line is for radar data corrected using mean VPRs, and the dashed line is from data corrected using locally identified VPRs. Figures 9a–c show rainfall accumulation from radar data recorded at 0.5°, 1.5°, and 2.5°, respectively. At far ranges, the range dependence of mean radar rainfall accumulation is weak but significant. Both of our VPR correction procedures reduce this range dependence. For the higher elevation angles (Figs. 9b,c), the range dependence of mean radar rainfall accumulation is more important and so is the benefit of the VPR correction procedures.

b. Evaluation using hourly radar and rain gauge data

In this and the following sections we use rain gauge data to assess the accuracy of the radar rainfall estimates and the improvement obtained using the different VPR correction method. Despite the conceptual problems associated with using rain gauges to evaluate radar estimates (Zawadzki 1982; Ciach and Krajewski 1999), we consider the differences between the collocated radar and gauge data to be a viable performance measure. Our main interest is in hourly rainfall accumulation as justified by the needs of hydrological modeling for catchments of about 500 km^2. We also consider daily rainfall accumulations and 2-yr totals. These larger integration times are of interest in climatological analyses.

We compare rain gauge hourly observations with the radar rainfall accumulation estimates from the closest radar pixel on the polar grid. Figure 10 shows the scatterplots of hourly rainfall accumulations stratified by the distance between the radar and the rain gauges. The three cases we show are for rainfall accumulations from radar data recorded at an elevation angle of 0.5° 1) after mean VPR-based correction, 2) after locally identified VPR-based correction, and 3) without VPR correction.

We used the root-mean-square (rms) of the difference between radar and a collocated gauge and the mean difference between radar and gauge (bias) to quantify the gain obtained using VPR correction procedures. The statistics are calculated, for each rain gauge, on hourly accumulations for those hours when both radar and rain gauge data are available. The results, stratified by range, are shown in Table 1. Considering all the gauges, the mean VPR-based correction lowers the mean rms from 0.77 to 0.73 mm (reduction of 5%). The locally identified VPR correction lowers the mean rms to 0.66 (reduction of 14%). The average hourly accumulation mean bias is 0.04 mm without VPR correction and is reduced to 0.01 mm with either of the VPR correction procedures.

The rms improvement we obtained underestimates the actual effect of the VPR schemes because the radar and rain gauge differences are due to two combined effects: 1) the natural variability of rainfall in space and 2) the radar rainfall estimation error that includes numerous sources of uncertainty. This issue is thoroughly dis-

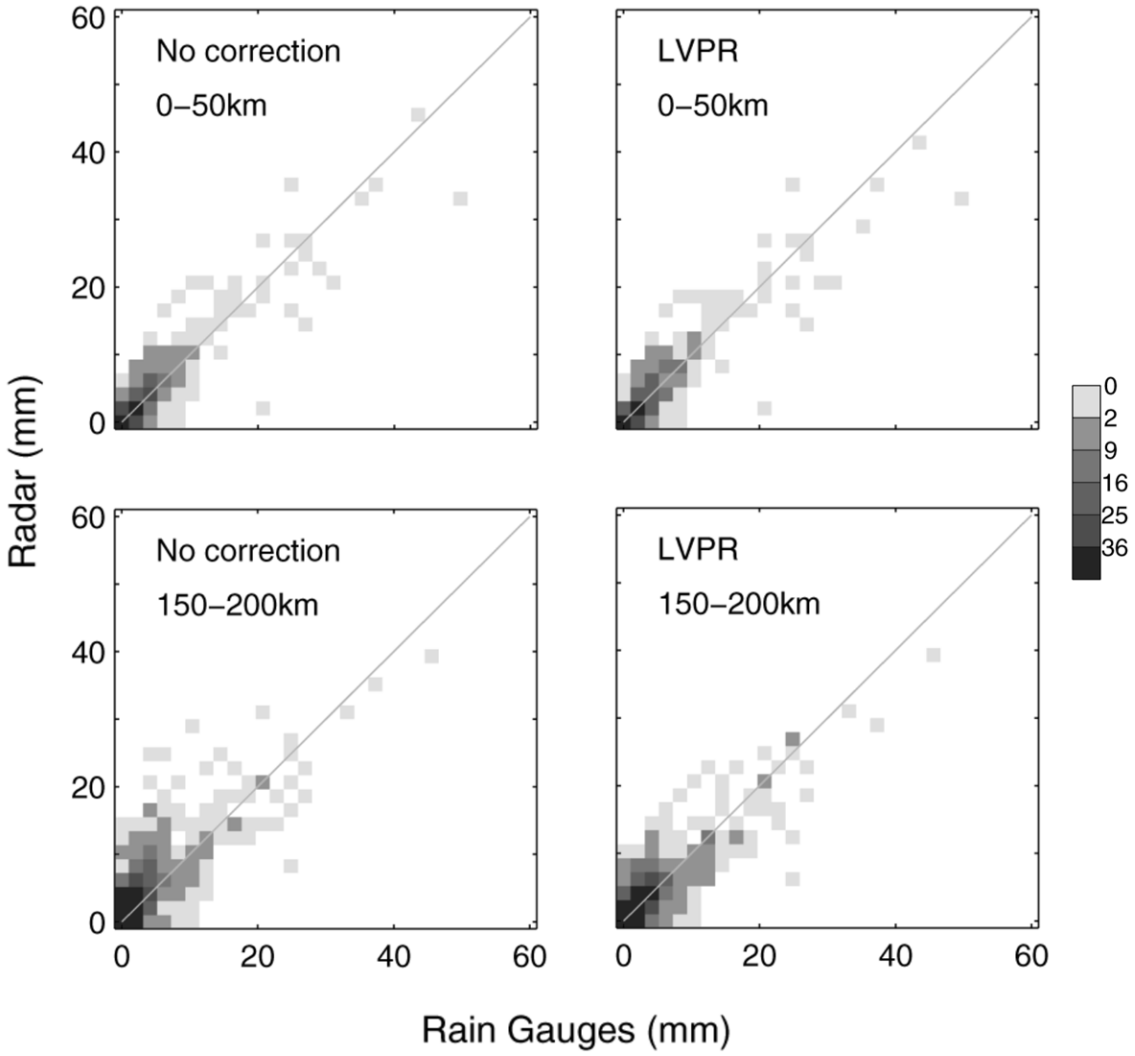

FIG. 10. Comparisons of hourly rainfall accumulations of gauges versus radar, organized by distance from the radar. The grayscale of the shading corresponds to the number of points in a given window of rain values. The window size is 2 mm.

cussed by Ciach and Krajewski (1999) who developed the error separation method (ESM) to deal with the problem. Following the ESM approach, Young et al. (2000) attempted to estimate the uncertainty of the hourly rainfall product used by the Tulsa River Forecast Office of the National Weather Service but concluded that they lack sufficient information about the small-scale variability of rainfall. Because our study uses similar rain gauge datasets, we do not attempt relevant analysis. Therefore, our estimate of rms error improvement is conservative.

The benefits of the VPR correction procedures are more obvious if we consider a reduction of the range dependence of the values of rms and bias. Without VPR correction, the values of rms (bias) are between 0.63 (−0.02), considering gauges between 50 and 100 km from the radar, and 0.91 mm (0.08 mm), considering gauges between 150 and 200 km from the radar. Thus, close to the radar, the VPR has little effect on the radar estimates. At far ranges (greater than 100 km), because of the VPR influence, radar rainfall values are often overestimated (see Fig. 13). This overestimation can be related to the brightband influence.

For mean VPR-based correction, the range dependence of the rms is reduced only until 150 km, whereas the bias is reduced for all ranges. The values of rms (bias) are between 0.62 (−0.03), for gauges between 50 and 100 km from the radar, and 0.69 mm (0.01 mm), for gauges between 100 and 150 km from the radar. Between 150 and 200 km, the MVPR-based corrections only marginally improve the accuracy of radar rainfall estimates in term of rms. This result comes from inaccurate corrections for some particular hours. At these distances, the MVPRs can induce large correction.

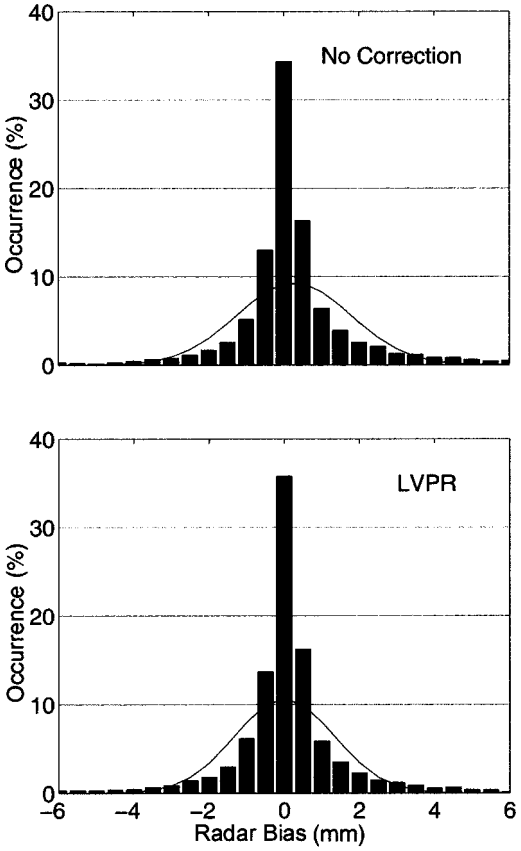

FIG. 11. Histogram of differences between radar and gauge hourly rainfall accumulation. The continuous line corresponds to the theoretical normal distribution having the same mean and variance as the studied sample.

When these corrections are inaccurate—for example, because of wide variations in VPR—a large error is introduced.

For LVPR-based corrections, the values of rms (bias) are between 0.62 (−0.03), for gauges between 50 and 100 km from the radar, and 0.74 mm (0.01 mm), for gauges between 150 and 200 km from the radar. For the gauges close to the radar (up to 100 km), the impact of VPR correction (Fig. 10) is weak. Far from the radar, the impact is more significant.

c. Statistical significance of the results

A valid question at this point is if the results we obtained demonstrate statistically significant improvement of radar rainfall estimation. Before we proceed to address this question we remind the reader that although we report both the bias and the root-mean-square difference, the goal of the VPR correction is to mitigate the systematic effect of range-dependent errors. Therefore, let us focus on the bias first. If the difference between the radar and rain gauge estimates were the errors of the radar algorithm (including the VPR correction) and if these differences were normally distributed, the significance of our results could be easily addressed using standard hypothesis testing tools. This is not the case, however. In Fig. 11 we show the histogram of the hourly differences for uncorrected and the LVPR-corrected data. For comparison. we show a normal distribution with the same mean and variance. Clearly, the fit is poor. However, the distribution is remarkably symmetric about the mean, suggesting that the first-order moment can be accurately estimated from even a much smaller sample. Indeed, we performed a simple resampling study that confirms it. From our sample of over 7000 radar–rain gauge hourly pairs (with at least one sensor recording rain) we randomly selected a subsample of 1000 pairs. We repeated this 1000 times, each time calculating the bias for the LVPR method. We plotted the distribution of the bias in Fig. 12. Note that almost 100% of the distribution is away from the uncorrected bias. Thus, there is little doubt that the improvement we obtained was due to the skill of the correction method.

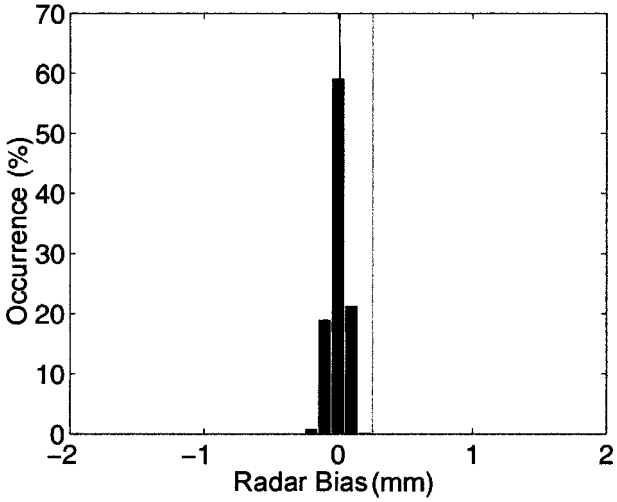

FIG. 12. The sampling distribution of the bias based on a resampling experiment using sample size of 1000. The gray vertical line shows the bias for the uncorrected data. The dark thin vertical line shows the bias obtained by the LVPR method.

Although discussion of the bias is the main point of our analysis, given that the rms reduction is not the goal of the VPR correction method, let us turn our attention to the rms differences. First, let us see the contribution of the rms reduction that is due to the bias reduction. The bias-adjusted rms for the distance class between 150 and 200 km is 0.9, indicating that the random effects dominate and the bias contributes little to the statistic. Thus, the rms reduction is due to the correction method. Could it be obtained by chance? To answer this question we could perform a resampling experiment similar to the one above, but it is not necessary. Because the comparisons before and after the correction use exactly the same rain gauge data, the effect of the gauge representativeness (sampling) error is constant. As we argued before, the existence of this error, which is random in

TABLE 1. Root-mean-square (and bias) of the difference between hourly, daily, and total accumulations from radar and gauge reflecting the improvement of rain estimates considering the two profile corrections and, for reference, without VPR correction.

Profile correction	Range from radar (km)			
	0–50	50–100	100–150	150–200
		Hourly accumulation (mm)		
Average rain gauge	0.34	0.38	0.31	0.30
Mean VPR	0.66 (0.03)	0.62 (−0.03)	0.69 (0.01)	0.89 (0.05)
Local VPR	0.65 (0.02)	0.62 (−0.03)	0.65 (0.01)	0.74 (0.01)
No correction	0.66 (0.03)	0.63 (−0.02)	0.78 (0.05)	0.91 (0.08)
		Daily accumulation (mm)		
Average rain gauge	4.11	4.65	3.81	3.64
Mean VPR	3.08 (0.36)	2.70 (−0.32)	3.13 (0.10)	4.15 (0.62)
Local VPR	2.93 (0.23)	2.60 (−0.36)	2.75 (0.04)	3.33 (0.42)
No correction	3.11 (0.34)	2.77 (−0.24)	3.88 (0.64)	4.95 (1.01)
		Total accumulation (mm)		
Average rain gauge	391.08	425.98	356.17	336.49
Mean VPR	51.33 (33.4)	47.38 (−31.6)	44.15 (8.9)	64.33 (59.2)
Local VPR	46.12 (22.1)	49.54 (−34.8)	39.89 (3.2)	44.20 (41.1)
No correction	49.1 (31.4)	45.1 (−21.3)	77.1 (71.2)	104.0 (89.2)

character, masks the actual rms reduction. If the effect of the natural rainfall variability is high, the improvement is more significant than that indicated by our results.

There is another way to argue our point. Because for the distances close to radar, that is, between 0 and 50 km, there is no need for the VPR correction, the rms for that range represents the rms due to effects not associated with the vertical structure of the reflectivity. If there were no VPR effect, this rms would increase with range, mainly because of the increasing gauge representativeness error as a result of the increasing sampling area of the radar. Thus, rms reduction due to VPR correction should not exceed such a limit. Indeed, the results of rms we obtained for distances between 50 and 200 km display a consistent behavior in this respect: they are reduced but do not fall below the value obtained for the closest range.

d. Evaluation using longer-scale rain accumulations

We also computed the values of rms and bias for daily and total rainfall accumulations (see Table 1). For daily accumulation, the gain achieved using VPR-based correction is more important. The rms is 3.85 mm without VPR correction, 3.31 mm (14% reduction) with mean VPR correction, and 2.89 mm (25% reduction) with LVPR correction. With larger timescales of accumulation, the problems we alluded to above of representativeness of gauges are less significant. So, too, are problems related to the choice of the *Z–R* relationship.

The larger timescales also reduce the effect of locally inaccurate VPR correction. The benefit of using LVPR instead of mean VPR is smaller than for hourly accumulations. The values of rms obtained considering total accumulation confirm this. The rms is 75 mm without VPR correction, 51 mm (32% reduction) with MVPR correction, and 44 mm (41% reduction) with LVPR correction. In this case, the benefit of using LVPR instead of MVPR probably is marginal.

We calculated the field of bias for the entire duration of our dataset by computing this bias gauge by gauge and interpolating between the locations of the gauges. The interpolation method is based on four-quadrant near neighbors and inverse distance weights—it is the same method used by the National Weather Service in its hydrologic forecasting. Figure 13 shows the maps of the bias (i) before quality control (QC) of the radar data, (ii) after QC, (iii) after QC and MVPR correction, and (iv) after QC and LVPR correction. The ''hot spot'' on the figure (about 145 km west of the radar) is most likely due to an underestimation by the gauge. This gauge (Red Rock, Oklahama, Mesonet code REDR) displays relatively long periods of reporting no rain during which radar observes rain. From these maps, it is clear that QC reduces the bias close to the radar (below 100 km), whereas the VPR correction does that at higher distances from the radar. This figure illustrates the benefit for each of these two steps and shows that, in terms of bias, data QC is as important as VPR correction.

We also evaluated radar rainfall estimates deduced from radar data recorded at higher elevation angles (1.5° and 2.5°). Our motivation was to study the situation when, because of total or partial occultation of the lowest beam, higher-elevation data must be used. This is often the case in mountainous regions. Because the VPR is more influential at higher elevation angles, the benefit of using a VPR correction should be more substantial. The results are shown in Table 2. For the radar data recorded at an elevation angle of 1.5°, the agreement between radar and gauge is weaker than that of radar data recorded at 0.5°. Between 0 and 100 km from the radar, radar data can be affected by the brightband influence (bias greater than 0 mm). At distances greater

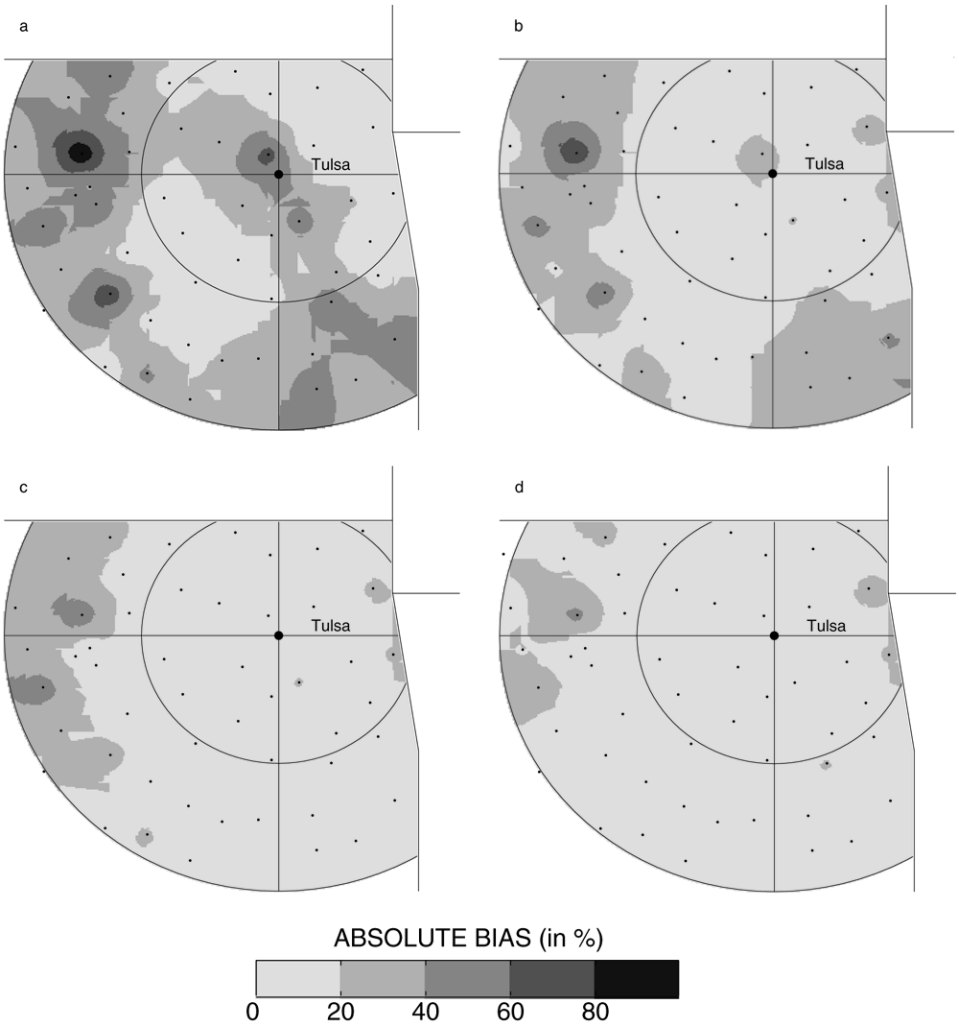

FIG. 13. Bias between radar and gauge total rainfall accumulation for radar data (a) before QC, (b) after QC, (c), after QC and MVPR correction, and (d) after QC and LVPR correction.

TABLE 2. Root-mean-square (and bias) of the difference between hourly rainfall accumulation from radar data (recorded at 0.5°, 1.5°, and 2.5° of elevation angle) and gauge.

	Range from radar (km)			
Profile correction	0–50	50–100	100–150	150–200
		0.5°		
Average rain gauge	0.34	0.38	0.31	0.30
Mean VPR	0.66 (0.03)	0.62 (−0.03)	0.69 (0.01)	0.89 (0.05)
Local VPR	0.65 (0.02)	0.62 (−0.03)	0.65 (0.01)	0.74 (0.01)
No correction	0.66 (0.03)	0.63 (−0.02)	0.78 (0.05)	0.91 (0.08)
		1.5°		
Mean VPR	0.65 (0.02)	0.73 (−0.01)	0.81 (0.01)	1.13 (0.01)
Local VPR	0.63 (0.02)	0.82 (−0.01)	0.76 (−0.01)	0.89 (−0.04)
No correction	0.72 (0.03)	1.30 (0.09)	0.92 (−0.04)	1.10 (−0.17)
		2.5°		
Mean VPR	0.79 (−0.01)	0.84 (−0.05)	0.89 (−0.07)	1.09 (−0.15)
Local VPR	0.71 (−0.01)	0.83 (−0.04)	0.94 (−0.09)	1.15 (−0.16)
No correction	1.06 (0.03)	1.15 (−0.04)	1.26 (−0.20)	1.41 (−0.24)

TABLE 3. Root-mean-square (and bias) of the difference between hourly rainfall accumulation from radar data and gauge for a warm and a cold season.

Profile correction	Range from radar (km)			
	0–50	50–100	100–150	150–200
		Cold season		
Average rain gauge	0.44	0.50	0.40	0.43
Mean VPR	0.77 (0.08)	0.68 (−0.01)	0.65 (−0.01)	0.94 (0.05)
Local VPR	0.75 (0.07)	0.67 (−0.01)	0.61 (0.01)	0.76 (0.04)
No correction	0.79 (0.08)	0.70 (0.01)	0.87 (0.09)	1.05 (0.12)
		Warm season		
Average rain gauge	0.27	0.30	0.26	0.21
Mean VPR	0.57 (−0.01)	0.58 (−0.04)	0.72 (0.02)	0.85 (0.05)
Local BPR	0.58 (−0.01)	0.58 (−0.04)	0.68 (0.01)	0.72 (0.03)
No correction	0.57 (−0.01)	0.58 (−0.04)	0.71 (0.03)	0.80 (0.06)

than 100 km, most of the time, the radar beam is above the melting layer (bias less than 0 mm). Without any correction, the rms is 1.06 mm (against 0.77 mm for radar data at 0.5°). The VPR correction procedure reduces the values of rms: 0.87 mm for the MVPR-based procedure and 0.80 mm for the LVPR-based procedure. These are weaker agreements than for 0.5°. This result reflects the limitations of the VPR correction procedures at far ranges (over 150 km considering this elevation angle). These limitation are due to (i) beam overshooting (no possible correction when the radar beam is above the echo top) and (ii) a better correlation of surface rainfall with water-coated frozen hydrometeors in the melting layer than with ice particles well above the freezing level (Seo and Breidenbach 1998). As a consequence, after VPR correction, radar data recorded at 1.5° provide ''accurate'' rainfall estimates only up to about 150 km. For radar data recorded at 2.5°, this range is further restricted to about 100 km.

e. Seasonal analysis

To investigate better the benefits and limitations of the VPR correction procedures, we performed a seasonal analysis. We divided data into a warm season (May–October), dominated by convective rainfall, and a cold season (November–April), dominated by widespread stratiform precipitation. Smith et al. (1996) proposed, for the same location, an extended warm season (from April to October). Considering our data and looking at the vertical structure of radar echoes, we find that April of 1994 and 1995 were dominated by widespread stratiform precipitation. Based on this observation, we included April into the cold season. One can expect a more important—but easier to correct—influence of the VPR for the cold season than for the warm season. The results of the comparison between radar and gauge, for both seasons, are presented in Table 3.

For the cold season, both VPR estimation procedures allow reducing the difference between radar and gauge. The rms (bias) is 0.87 mm (0.08) without VPR correction, 0.76 (0.02) using the MVPR-based procedure (reduction of 13% of the rms), and 0.68 (0.01) using the LVPR-based procedure (reduction of 22% of the rms). For the cold season, the MVPR-based procedure reduces the difference between radar and gauge as far as 200 km from the radar, although the improvement is insignificant beyond 150 km.

For the warm season, only the LVPR-based procedure allows reducing the difference between radar and gauge in terms of rms, and both methods in terms of bias. The rms (bias) is 0.69 mm (0.01 mm) without VPR correction, 0.70 (0.01 mm) using the MVPR-based procedure, and 0.65 (0.01 mm) using locally identified VPR. These results show that it is more difficult to correct for the VPR influence for the warm season. In particular, the MVPR-based procedure increases (in term of rms) the difference between radar and gauge at distances greater than 100 km from the radar.

6. Conclusions and outlook

We described an evaluation of two methods of correcting the vertical profile of reflectivity in WSR-88D radar data and the corresponding improvements in rainfall estimates. Using two years of data from the WSR-88D in Tulsa and the Oklahoma Mesonet rain gauge database, we compared the two methods according to several criteria applied at various temporal scales of integration. The first method to determine the VPR is similar to the one used operationally in Switzerland and provides mean VPR obtained from radar data at close ranges. The second method provides locally identified VPR for areas of about 20 km by 20 km.

Because the VPR induces range-dependent errors in long-term accumulation of rainfall, both correction methods aim to reduce them. We found slightly better results using the locally identified VPR. Both methods reduce significantly the bias between radar and gauge daily and hourly rainfall estimates. Both also reduce the rms error, but here the performance of the locally identified VPR is much better. The difference between the

two methods, however, decreases as the timescale increases.

We also found that the VPR is more influential and a correction is more effective during the cold season and for lower rainfall intensities than for the warm season and larger rainfall intensities. Last, we briefly investigated the influence of the natural variability of rainfall on our comparison between radar and gauge. Because we lack adequate information on small-scale rainfall variability, we did not perform a comprehensive investigation. However, because the effect of natural variability is range dependent (as the radar averaging area increases with distance from radar), it interfered with our results. This influence of the natural variability of rainfall has to be accounted for to obtain a representative influence of the VPR corrections.

As a by-product of the study, we obtained a climatic mean VPR, which can be used for radar rainfall error parameterization or error evaluation purposes. Another potential application is related to short-term rainfall forecasting methods. Some of the models used require estimates of the vertically integrated rainwater content, which can be deduced from the VPRs (see, e.g., French and Krajewski 1994).

Based on our study, we conclude that both of the methods we investigated have serious shortcomings as far as being considered for operational real-time application. The mean VPR method can lead to large inappropriate corrections. The locally identified VPR method is very expensive in terms of computer memory allocation (3 times more than the other method) and computer time needed (about 10 times more). A compromise method, specifically dedicated to WSR-88D rainfall estimates and proposed by Seo et al. (2000), takes into account the smoothing effect of beam widening and is computationally efficient. We are currently conducting a long-term evaluation of this method and will report results in the near future.

Still, the method does not take into account the geographical variability of the VPR as the LVPRs do. One way to address this problem partially is to define criteria governing when to apply the corrections associated with the mean VPR based on some sort of classification of the radar echoes [e.g., stratiform vs convective; see Steiner et al. (1995)] and to estimate independently the associated VPRs. The idea is to capture the main geographical variations of the VPR.

We did not use optimized algorithms for rainfall estimation. Optimal setting of the *Z–R* relationship and other parameters, along with a preclassification of rainfall, should further improve our results.

Acknowledgments. This study was supported under the Cooperative Agreement between the Office of Hydrology of the National Weather Service (NWS) and the Iowa Institute of Hydraulic Research (NA47WH0495). We thank Dr. Dong-Jun Seo of NWS for many valuable comments in the course of this study. We are grateful to the Oklahoma Climatological Survey and the Oklahoma EPSCoR program for providing the rain gauge data from the Oklahoma Mesonet. We also thank Dr. Keith Brewster and Dr. Efi Foufoula-Georgiou for their helpful comments on an earlier version of the paper.

REFERENCES

Andrieu, H., and J. D. Creutin, 1995: Identification of vertical profiles of radar reflectivity for hydrological applications using an inverse method. Part I: Formulation. *J. Appl. Meteor.,* **34,** 225–239.

——, G. Delrieu, and J. D. Creutin, 1995: Identification of vertical profiles of radar reflectivity for hydrological applications using an inverse method. Part II: Sensitivity analysis and case study. *J. Appl. Meteor.,* **34,** 240–259.

Austin, P. M., 1987: Relation between measured radar reflectivity and surface rainfall. *Mon. Wea. Rev.,* **115,** 1053–1070.

Brock, F. V., K. C. Crawford, R. L. Elliott, G. W. Cuperus, S. J. Stadler, H. L. Johnson, and M. D. Eilts, 1995: The Oklahoma Mesonet: A technical overview. *J. Atmos. Oceanic Technol.,* **12,** 5–19.

Ciach, J. G., and W. F. Krajewski, 1999: On the estimation of radar rainfall error variance. *Adv. Water Resour.,* **22,** 585–595.

French, M. N., and W. F. Krajewski, 1994: A model for real-time quantitative rainfall forecasting using remote sensing. 1. Formulation. *Water Resour. Res.,* **30,** 1075–1083.

Fulton, R. A., J. P. Breidenbach, D.-J. Seo, D. A. Miller, and T. O'Bannon, 1998: The WSR-88D rainfall algorithm. *Wea. Forecasting,* **13,** 377–395.

Grecu, M., and W. F. Krajewski, 1999: Anomalous pattern detection in radar echoes by using neural networks. *IEEE Trans. Geosci. Remote Sens.,* **37,** 287–296.

Houze, R. A., Jr., 1993: *Cloud Dynamics.* Academic Press, 573 pp.

——, B. F. Smull, and P. Dodge, 1990: Mesoscale organization of springtime rainstorms in Oklahoma. *Mon. Wea. Rev.,* **118,** 613–654.

Joss, J., and R. Lee, 1995: The application of radar–gauge comparisons to operational precipitation profile corrections. *J. Appl. Meteor.,* **34,** 2612–2630.

Kitchen, M., R. Brown, and A. G. Davies, 1994: Real-time correction of weather radar data for the effects of bright band, range and orographic growth in widespread precipitation. *Quart. J. Roy. Meteor. Soc.,* **120,** 1231–1254.

Klazura, G. E., and D. A. Imy, 1993: A description of the initial set of analysis products available from the NEXRAD WSR-88D system. *Bull. Amer. Meteor. Soc.,* **74,** 1293–1311.

Krajewski, W. F., and B. Vignal, 2001: Evaluation of anomalous propagation echo detection in WSR-88D data: A large sample case study. *J. Atmos. Oceanic Technol.,* **18,** 807–814.

Kruger, A., and W. F. Krajewski, 1997: Efficient storage of weather radar data. *Software Pract. Exper.,* **27,** 623–635.

Menke, W., 1989: *Geophysical Data Analysis: Discrete Inverse Theory.* Academic Press, 260 pp.

Seo, D.-J., J. Breidenbach, R. Fulton, D. Miller, and T. O'Bannon, 2000: Real-time adjustment of range-dependent biases in WSR-88D rainfall estimates due to nonuniform vertical profile of reflectivity. *J. Hydrometeor.,* **1,** 222–240.

Shafer, M. A., C. A. Fiebrich, D. S. Arndt, S. E. Fredrickson, and T. W. Hughes, 2000: Quality assurance procedures in the Oklahoma Mesonetwork. *J. Atmos. Oceanic Technol.,* **17,** 474–494.

Smith, J. A., D.-J. Seo, M. L. Baeck, and M. D. Hudlow, 1996: An intercomparison study of NEXRAD precipitation estimates. *Water Resour. Res.,* **32,** 2035–2045.

Smyth, T. J., and A. J. Illingworth, 1998: Radar estimates of rainfall rates at the ground in bright band and non-bright band events. *Quart. J. Roy. Meteor. Soc.,* **124,** 2417–2434.

Steiner, M., R. A. Houze Jr., and S. E. Yuter, 1995: Climatological characterization of three-dimensional storm structure from operational radar and rain gauge data. *J. Appl. Meteor.*, **34,** 1978–2007.

Tarantola, A., and B. Valette, 1982a: Generalized nonlinear inverse problem solved using the least squares criterion. *Rev. Geophys. Space Phys.*, **20,** 219–232.

——, and ——, 1982b: Inverse problems: Quest for information. *J. Geophys. Space Phys.*, **50,** 159–170.

Vignal, B., H. Andrieu, and J. D. Creutin, 1999: Identification of vertical profiles of reflectivity from volume-scan radar data. *J. Appl. Meteor.*, **38,** 1214–1228.

——, G. Galli, J. Joss, and U. Germann, 2000: Three methods to determine profiles of reflectivity from volumetric radar data to correct precipitation estimates. *J. Appl. Meteor.*, **39,** 1715–1726.

Young, C. B., A. A. Bradley, W. F. Krajewski, A. Kruger, and M. L. Morrissey, 2000: Evaluating NEXRAD multisensor precipitation estimates for operational hydrologic forecasting. *J. Hydrometeor.*, **1,** 241–254.

Zawadzki, I., 1982: The quantitative interpretation of weather radar measurements. *Atmos.–Ocean*, **20,** 158–180.